Droplet diameter, flux, and total current measurements in an electrohydrodynamic spray

Patrick F. Dunn and Stephen R. Snarski
Particle Dynamics Laboratory, Department of Aerospace and Mechanical Engineering, University of Notre Dame, Notre Dame, Indiana 46556

(Received 18 June 1991; accepted for publication 1 October 1991)

The measured diameter and flux distributions and total current of ethanol droplets generated electrohydrodynamically from a single hypodermic needle at two different spray charge densities are presented and discussed. The resultant droplet diameter and droplet flux distributions reveal a progressive production of an increasing number of smaller diameter droplets with increasing spray charge density. These are consistent with observations made of the filament breakup-to-droplet process in this region. The droplet flux distributions are used to construct droplet charge flux distributions by assuming various models of the droplet charging process. The resultant charge fluxes are logarithmically related to lateral position, regardless of the droplet charging model assumed. The integrals of the various charge flux profiles are compared to the measured total current. This approach reveals the best agreement between measured and predicted total droplet currents when an equilibrium end-state process for droplet charging is assumed.

I. INTRODUCTION

With the recent development of advanced *in situ* laser diagnostic systems, it is now possible to obtain nonintrusive measurements of the velocity and/or diameter of droplets within electrohydrodynamic (EHD) sprays to a level of detail that was not possible in earlier studies. This paper presents the results of such laser diagnostic measurements of droplet diameter and flux within a single EHD spray. The present work further examines the process of droplet charging by using the various models that relate droplet diameter and charge to predict the total droplet current, which also is measured. As a consequence, the model that best describes the charging process for these experiments can be identified. The major findings from this study, when considered in conjunction with those reported recently by Dunn and Snarski[1] conducted under similar conditions using two parallel needles, support that droplet sprays of ethanol obtained at the subject levels of spray charge density closely approach or already have reached their equilibrium end state, as described by Kelly.[2]

II. EXPERIMENTS

In the present experiments, a fine spray of droplets in the approximate diameter range of 1–50 μm were generated electrohydrodynamically by supplying ethanol at a fixed mass flow rate (4.5 mg/s) from a syringe pump and applying a high positive voltage to a stainless-steel hypodermic needle (216 μm i.d., 406 μm o.d., 1.905 cm length) located 38 cm above an electrically grounded droplet-collection funnel (see Fig. 1). Droplet diameter and flux distributions were obtained using a phase Doppler particle analyzer (PDPA) (see Bachalo and Houser[3]) at two axial (z) positions below the needle's tip (15 and 30 mm), at approximately 20 lateral (x) positions for each axial position and at four applied voltages (15, 20, 25, and 30 kV). Total droplet currents were measured as the collected droplet current to ground through an electrometer. The resultant spray charge densities for these conditions were 12, 42, 106, and 210 C/m^3, respectively. A description of the experiment's main components and operating procedure is presented in further detail elsewhere.[1]

Only the measurements acquired at the two highest spray charge densities and first axial position are presented and discussed herein. These essentially constitute those measurements in the fine spray mode (see Snarski[4] for a discussion of the various EHD regimes encountered in such experiments) in which micrometer-size droplets are produced from short, brushlike filaments emanating directly from the tip of the needle. This situation is achieved at relatively high spray charge densities (in the range of $\sim$100–200 C/m^3), at which the electric-field strength at the tip of the needle is $\sim 10^6$ V/m.

Estimated uncertainties in the measured quantities were 10% for the volumetric flow rate and less than 1% for the measured voltage. The uncertainty for the probe volume location also was less than 1%, while the typical uncertainty in the measured diameter was 4%, as estimated by Bachalo and Houser.[3] The overall range of uncertainty in the measured diameter for those measured in the present experiments was from 2% to 16%, based upon the PDPA droplet sizing calibration studies of O'Hern, Rader, and Ceman.[5] Uncertainties in the current measurement were determined from Snarski's estimates[4] to be approximately 10% and 25% for the two high-charge-density cases reported herein. The best estimates of the current measurements at the higher voltages that are reported herein were obtained by extrapolating those measured at the lower voltages and at the same needle-to-funnel distance and those at the higher voltages but at different needle-to-funnel distances.

 0021-8979/92/130080-05$04.00

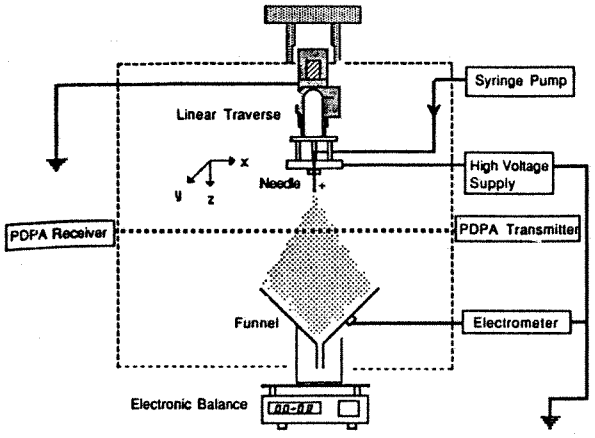

FIG. 1. Schematic drawing of the experiment.

III. RESULTS AND DISCUSSION

The droplet diameter distributions measured at the 15-mm axial position for the spray charge densities of 106 and 210 C/m^3 are shown in Fig. 2 for three lateral positions. These lateral positions, representing typical axial centerline ($x = 0$ mm), near-centerline ($x = 8$ mm), and peripheral ($x = 32$ or 36 mm) distributions, adequately display the evolution of distributions that occurred across the span of the axially symmetric spray. At the lower charge density, the distributions at the centerline and peripheral locations are reasonably similar, but both are somewhat different than that at the near-centerline location. The mode of the distribution (the diameter of maximum count) is smallest at the centerline. At the higher charge density, the distributions become comparatively more disparate and evolve toward a lognormal distribution at the centerline. A comparison of the distributions between the two spray charge densities reveals a progressive increase with increasing spray charge density in the number of smaller droplets occurring at the centerline and at the periphery. This is especially evident at the axial centerline. This trend is like that obtained previously by Snarski[4] in similar experiments using two needles.

Individual droplet size distributions can be modeled by various empirical fits (see Lefebvre[6]). For the present study, the Rosin–Rammler distribution provided excellent agreement with the measurements. In particular, the measured and predicted volume mean diameters agreed to within approximately 5% for all cases and to within approximately 2% when averaged over the lateral span of the spray. A comparison between measured and predicted percent droplet volume and count distributions is given in Fig. 3. The resultant values for the two Rosin–Rammler fit parameters (the size dispersion coefficient q and the diameter of 63.2% cumulative liquid volume X) at a fixed spray charge density were minimum at the centerline and increased by approximately 10%–20% across the lateral span of the spray. When averaged across the spray, these values plus or minus their standard deviations were $q_{avg} = 3.65 \pm 0.27$ and $X_{avg} = 26.6 \pm 1.80$ μm for 106 C/m^3 and $q_{avg} = 3.52 \pm 0.18$ and $X_{avg} = 22.5 \pm 1.90$ μm for 210 C/m^3. These resultant values are within the bounds of those obtained for most sprays[6] and are like those found in Snarski's experiments.[4] Also, the parameters q and X were minimum at the spray centerline at each charge density, implying a diameter distribution of smaller droplets with slightly more dispersion than at other locations. This occurred even more so at the higher spray charge density.

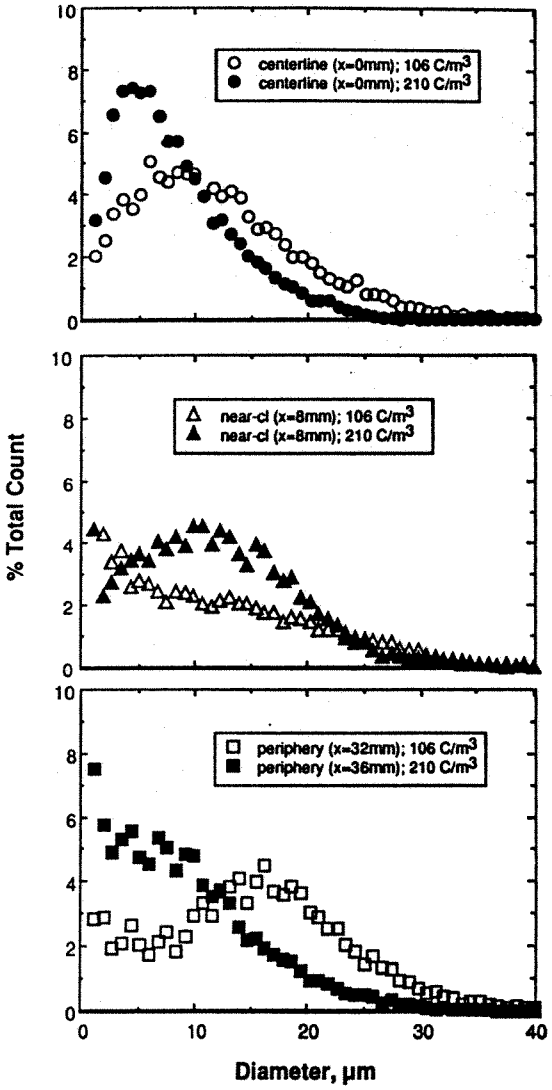

FIG. 2. Droplet diameter distributions at the 15-mm axial location and spray charge densities of 106 and 210 C/m^3.

At the higher charge density, however, a progressively larger number of smaller diameter droplets comprised a majority of the droplet population. For this situation, the Rosin–Rammler empirical fit inherently did not predict well the lower-diameter end of the distribution. Here, the measured diameter distribution was better described in this region by a lognormal fit, as evidenced by the precision of the lognormal fit of the count distribution shown in Fig. 3. Based upon this trend, it is plausible to expect that at even higher charge densities a normal distribution will provide the best fit, as predicted by Kelly,[2] if the droplets reach an equilibrium end state. Such an evolution to a normal dis-

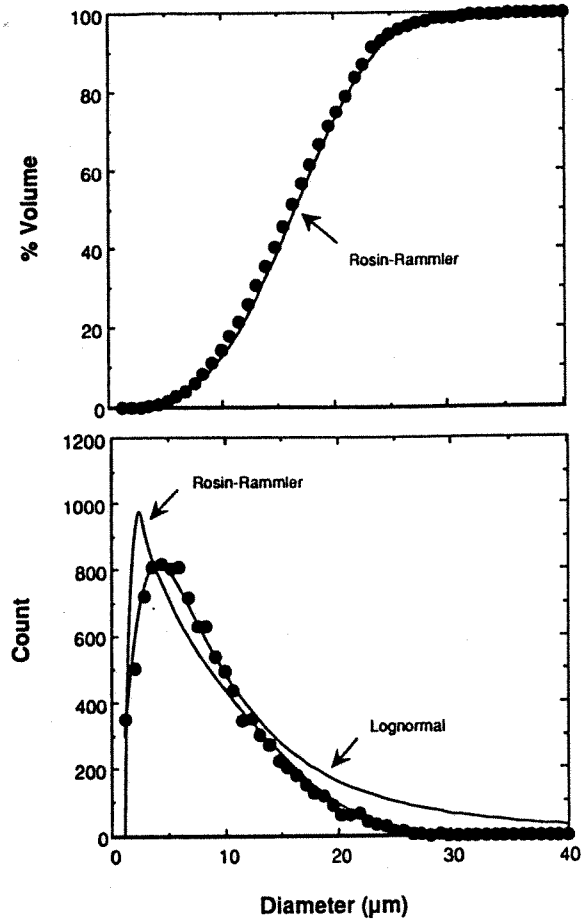

FIG. 3. Rosin–Rammler and lognormal fit comparison at the spray centerline, 15-mm axial location and spray charge density of 210 C/m^3.

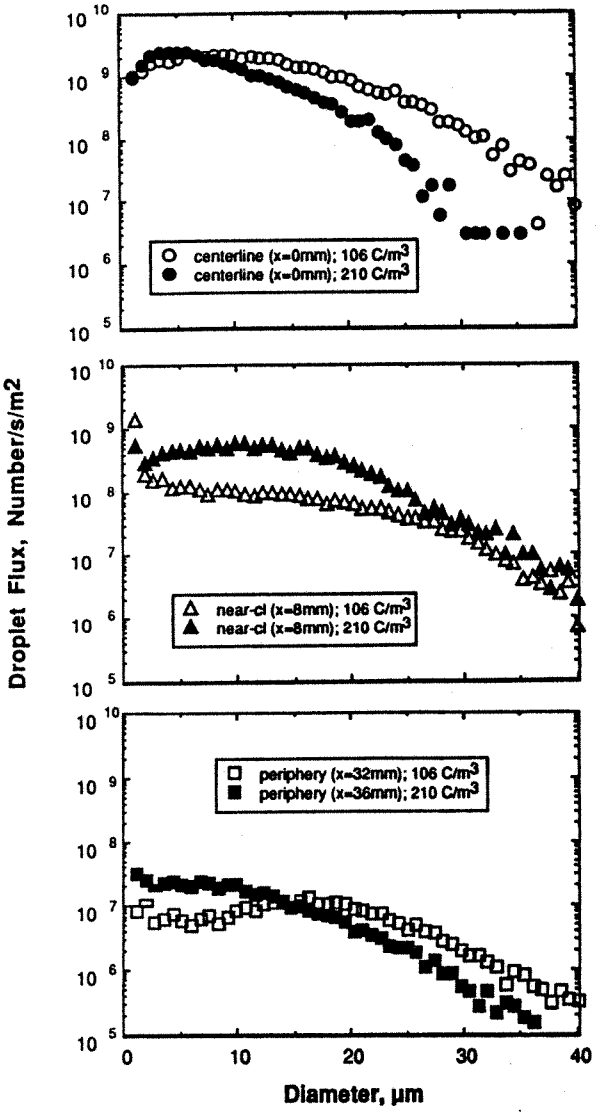

FIG. 4. Droplet flux distributions at the 15-mm axial location and spray charge densities of 106 and 210 C/m^3.

tribution would signify a reduction in the complexity of or number of parameters affecting the droplet population.[7]

Further insight into the dynamics of the droplets within the spray can be gained by examining the measured droplet flux distributions. These are presented in Fig. 4 for the same conditions as those in Fig. 2. At a fixed spray charge density, the greatest droplet flux occurred at the centerline where the droplet population was comprised of a majority of small droplets. In the lateral direction toward the periphery of the spray, the droplet flux decreased appreciably, eventually by two to three orders of magnitude at the periphery. At the higher charge density, for all lateral positions, the maximum value of the droplet flux occurred at smaller diameters.

The aforementioned droplet diameter and droplet flux distributions and their noted changes with increasing charge density are consistent with the droplet production mechanism of the fine spray mode. Observations of the droplet formation process (e.g., as recorded by Snarski[4]) have established that they are produced by the instability breakup of brushlike filaments extending from the tip of the needle. At the lower charge density examined in this mode, these filaments are relatively thin (ranging from approximately $\frac{1}{2}$–$\frac{1}{20}$ of the needle i.d.) and approximately ten in number. With increasing charge density, the length and diameter of the filaments decrease and their number increases, thereby producing a larger number of relatively smaller droplets.

It is plausible that as these droplets move toward the collection funnel and undergo some evaporation that they could reach their Rayleigh charge limit and consequently disrupt into smaller droplets. This subsequently would yield a smaller droplet population. At present, however, there has been no quantitative evidence presented in the literature for Rayleigh breakup in this spray regime. As will be discussed later, evidence gained from the correlations of velocity and diameter measurements support that droplet charging never reaches the Rayleigh limit in the subject region of measurement. Thus, based upon the evidence in hand, the smaller droplets produced in the subject measurement region near the needle with increasing charge density are probably the result of the instability breakup of filaments and not of the Rayleigh limit disruption of parent droplets.

The measured droplet flux distributions also can be used in conjunction with various models that relate droplet charge to diameter to construct charge flux distributions. This is done by incorporating a droplet charge-to-diameter relation into the droplet flux distribution, directly yielding the charge flux distribution. By subsequently comparing the integral of the resultant charge flux distribution over the entire cross section of the spray to the measured total droplet current, the droplet charging model most appropriate for these experiments can be identified.

There already is some evidence that the droplet charging model for this type of experiment is that in which droplet charge is directly proportional to diameter. This is found in two recent independent studies in which the correlations of measured droplet velocities and diameters were reported. For the case of two interacting EHD ethanol sprays in the fine spray mode, Dunn and Snarski[1] have presented measurements that show no significant correlation between velocity and diameter in the region of interest. A similar finding was obtained from the correlations of measurements by Gomez and Tang[8] for the case of a single methanol electrospray in the stable jet mode. As can be shown by examining the droplet's governing momentum equation, this lack of correlation directly implies that droplet charge must be proportional to diameter in the subject measurement region of the spray.

Implicit in the present approach is the assumption that the total droplet charge remains constant between the measurement location of the diameter distribution (either $z = 1.5$ or 3.0 cm) and that of the total current ($z = 38$ cm). In this light, it is necessary to consider how possible in-flight droplet evaporation between these two locations affects this assumption. It is difficult to determine readily the extent of droplet evaporation, primarily because of estimating the increase in local vapor concentration during transit within the droplet cloud. However, the droplet transit time between these locations over which evaporation can occur can be estimated. An analysis that considers the electrical, gravitational, and drag forces acting on the droplet in this region (see Snarski and Dunn[9]) reveals that the droplet velocity will relax immediately to its terminal velocity (based upon its electrical mobility) as dictated by the local electric field. This, for the present experiments, yields transit times between the two locations ranging from approximately 100 to 500 ms. These times are comparable to the lifetimes of ethanol droplets in vapor-free air,[10] which is a conservative overestimate. Thus, it is likely that some evaporation has occurred for all the droplets in the subject diameter range. This, however, does not affect the initial assumption unless some loss in droplet charge occurs as a result of this process.

Evaporation *per se*, however, does not affect the assumption of constant total droplet current. Present evidence supports that there is no loss of droplet charge during evaporation. This was shown by the experiments of Abbas and Lantham,[11] in which the electrical charge on water, aniline, and toluene droplets in the 60–400-μm-diam range was found to remain constant during evaporation. This was so even for sibling droplets produced when the droplet charge exceeded the Rayleigh limit.

Charge, however, can be lost indirectly as a result of evaporation. This occurs when some droplets are reduced in size by in-flight evaporation to the extent that they are repelled laterally from the spray and miss the collection funnel. This type of spray broadening near the funnel has been observed at high spray charge densities and reported by Snarski. He conservatively estimated the loss in droplet current to range from approximately 1% at the lowest charge density that he examined (59 C/m^3) to approximately 30% at the highest charge density (278 C/m^3). Hence, it is valid to assume for the present experiments that droplet charge is retained during evaporation, but that some of the total droplet current is lost by the concomitant spray broadening. This yields an uncertainty in the droplet current of approximately 10% and 25% (based upon Snarski's estimates) for the two charge-density cases (106 and 210 C/m^3) reported herein.

In the present study, several droplet charging models were examined. These included those in which charge is proportional to diameter$^{3/2}$ [the minimum, most probable and maximum (Rayleigh limit) charging states, as described by Pfeifer and Hendricks[12]] and that in which charge is proportional to diameter (the equilibrium end state, as presented by Kelly.[2]) Analytically, the models are $q = k\sqrt{8\pi^2\epsilon_0\gamma d^{3/2}}$ and $q = [2\pi\epsilon_0(-\alpha'/\beta')/e]d$, in which q is the charge, d the diameter, ϵ_0 the permittivity of free space (8.854×10^{-12} F/m) which closely approximates that in air, γ the surface tension, e the elemental charge (1.602×10^{-19} C), $(-\alpha'/\beta')$ the characteristic electrospray energy ($\sim0.85\times10^{-17}$ J), and $k = 1.0$, 0.50, and 0.22 for the maximum, most probable, and minimum charging states, respectively. The maximum charge results when the electrical force as a result of charge on the droplet's surface equals the surface tension force. The most probable charge is found when the total energy of the droplet population is minimized. The minimum charge is a consequence of the constraint that the total energy of the droplet population cannot exceed the maximum possible total charge of the population produced by the disruption of a parent drop. The charge present at the equilibrium end state is derived by assuming that charge is distributed with equal probability among all available droplets in accordance with Fermi–Dirac statistics.

The resultant droplet charge flux profiles at both charge densities are displayed in Fig. 5 for each of the Rayleigh (maximum charge) and Kelly (equilibrium end state) models. Implicit in determining these profiles is the choice of a diameter that is representative of the diameter distribution at each lateral position. Here, for the Rayleigh model, the PDPA measured diameters were used directly and, for Kelly's model, several representative diameters were examined (d_{mode}, d_{10}, d_{20}, d_{30}, and d_{32}—see Lefebvre[6]). The linear average diameter d_{10} gave the best agreement between experiment and theory in terms of total current measurement. At both spray charge densities, each model predicted that the maximum charge flux was at the centerline. The Rayleigh model, as anticipated, predicted the highest charge flux. Comparison between the two

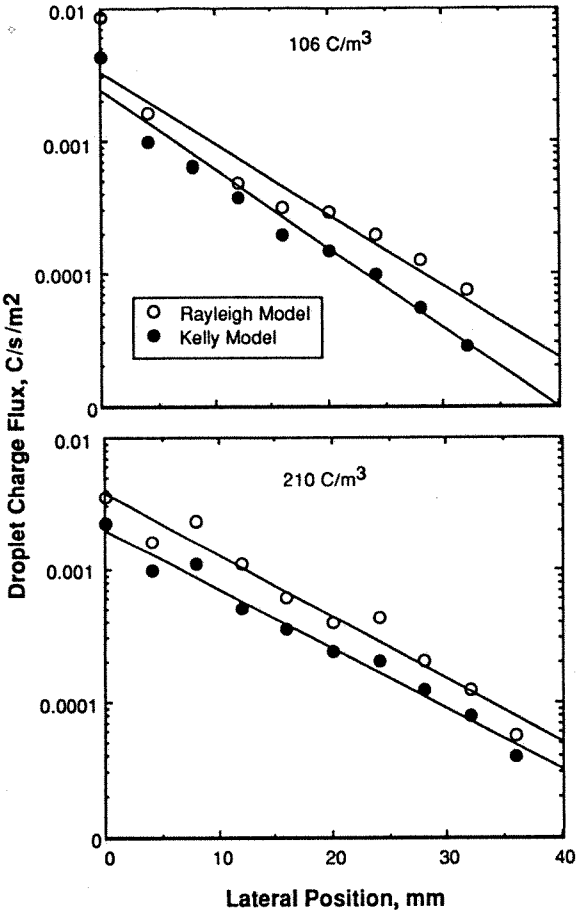

FIG. 5. Droplet charge flux profiles for Rayleigh's and Kelly's models at the 15-mm axial location and spray charge densities of 106 and 210 C/m^3.

charge-density cases further showed that the droplet charge flux distribution with increasing spray charge density became logarithmically related to lateral position. The least-squares fits of the data yielded high correlation coefficient values of 0.98 and 0.99 at the higher charge density and 0.94 and 0.94 at the lower charge density for the Rayleigh and Kelly models, respectively. All of these values corresponded to confidence levels greater than 99.9% when considering the number of lateral positions examined. These findings imply, regardless of the droplet charging model assumed, that the droplet charge flux distribution is logarithmically related to lateral position.

The model most descriptive of the present experiments can be identified by numerically integrating these profiles across the lateral span of the spray to yield values that can be compared to the measured total droplet current. The predicted total currents also can be determined for the most probable and minimum charging models by noting that they are simply 50% and 22% of that for the Rayleigh model. The results of this comparison are presented in Table I. This comparison revealed agreement to within the experimental uncertainty with the most probable charge model of the minimum energy theory and the equilibrium end-state model of the minimum entropy theory (to within approximately 7% and 5%, respectively, for the lower-charge-density case and to within approximately 16% and 22%, respectively, for the higher-charge-density case). The total droplet currents predicted from Rayleigh's model were approximately twice the magnitude of the measured currents; those predicted by the minimum charging model were approximately one-half. When considered in conjunction with the aforementioned findings of the velocity-diameter correlation measurements, these results support that the equilibrium end-state model most appropriately describes the present experimental results.

TABLE I. Total droplet current: Measured vs predicted. I_m: measured current; I_1: maximum current; I_2: most probable current; I_3: minimum current; I_4: equilibrium end-state current; all in units of μA.

C/m^3	I_m	I_1	I_2	I_3	I_4
106	0.60	1.27	0.64	0.28	0.63
210	1.20	2.08	1.04	0.46	0.94

IV. CONCLUSIONS

The measurements presented herein support that droplet sprays of ethanol obtained at the subject levels of spray charge density closely approach or may have already reached their equilibrium end state. This conclusion was drawn from the observed evolution of the droplet diameter and flux distributions with increasing spray charge density. Further evidence was acquired by determining that the best agreement between measured and predicted total droplet currents was achieved by assuming an equilibrium end-state process for droplet charging.

ACKNOWLEDGMENTS

This work was performed under MIPR Grant No. FY76168800343 between the University of Chicago and the Department of Defense and under Contract No. 62622401 between Argonne National Laboratory and the University of Notre Dame. We gratefully acknowledge our technical contacts within the Engineering Physics Division of Argonne National Laboratory (Dr. V. J. Novick, program coordinator, and Dr. E. D. Doss, program manager). The experiments reported herein were part of the graduate research of S.R.S. conducted in the Particle Dynamics Laboratory in the Department of Aerospace and Mechanical Engineering at the University of Notre Dame.

[1] P. F. Dunn and S. R. Snarski, Phys. Fluids A 3, 492 (1991).
[2] A. J. Kelly, J. Appl. Phys. 47, 5264 (1976).
[3] W. D. Bachalo and M. J. Houser, Opt. Eng. 23, 583 (1984).
[4] S. R. Snarski, masters thesis, University of Notre Dame, Notre Dame, IN, 1988.
[5] T. J. O'Hern, D. J. Rader, and D. L. Ceman (unpublished).
[6] A. H. Lefebvre, *Atomization and Sprays* (Hemisphere, New York, 1989).
[7] B. J. West and M. Shlesinger, Am. Sci. 78, 40 (1990).
[8] A. Gomez and K. Tang (unpublished).
[9] S. R. Snarski and P. F. Dunn, Exp. Fluids 11, 268 (1991).
[10] W. C. Hinds, *Aerosol Technology* (Wiley, New York, 1982).
[11] M. A. Abbas and J. Latham, J. Fluid Mech. 30, 663 (1967).
[12] R. J. Pfeifer and C. D. Hendricks, Phys. Fluids 10, 2149 (1967).